AN UPPER BOUND SOLUTION FOR THE EQUAL-CHANNEL ANGULAR PRESSING PROCESS

Neil de Medeiros
Universidade Federal Fluminense - Escola de Engenharia Industrial Metalúrgica de Volta Redonda
Av. dos Trabalhadores, nº:420, Volta Redonda, RJ, 27255-125, Brazil
neil@metal.eeimvr.uff.br

Luciano Pessanha Moreira
Universidade Federal Fluminense - Escola de Engenharia Industrial Metalúrgica de Volta Redonda
Av. dos Trabalhadores, nº:420, Volta Redonda, RJ, 27255-125, Brazil
luciano.moreira@metal.eeimvr.uff.br

Abstract. *In the present work we report an analytical solution for the equal-channel angular pressing (ECAP) process. This solution is based upon the upper bound method considering nonlinear material work-hardening, the friction behaviour and different fillet radii located at the die intersection channels. First of all, the dependence of the ECAP pressing pressure and the effective plastic strain obtained for a single pass are analyzed as a function of the friction factor and the die fillet radii. For comparison purposes, the predictions of the present model are first compared with the analytical solution proposed by Eivani and Karimi Taheri [J. Mat. Proc. Tech., 182 (2007) 555]. Afterwards, the experimental ECAP load data obtained by Eivani and Karimi Taheri for an Al-6070 billet are compared to the forecasted values determined with the present model. The results point out the influence of the die fillet radii upon the normalized ECAP pressure, independently of the friction factor adopted. As one may expect, the most severe condition is achieved when either the inner and outer fillet radii are equal to zero. For a fixed inner die fillet radius value, the proposed solution shows a more pertinent dependence of the ECAP pressure than the solution proposed by Eivani and Karimi Taheri. Finally, the present model can be viewed as general since it provides more realistic results for the Al-6090 experimental ECAP loading due to inclusion of the complete die geometrical effects on the upper bound solution of the normalized pressing pressure.*

***Keywords**: Upper Bound Method, Severe Plastic Deformation, Equal Channel Angular Pressing.*

1. INTRODUCTION

The equal channel angular pressing (ECAP) is a severe plastic deformation technique to produce bulk ultra-fine grained materials with improved mechanical properties, see the works of Segal (1995), Valiev *et al.* (2000) and most recently by Valiev and Langdon (2006), Zhao *et al.* (2006) and Zhang *et al.* (2007). In this technique, a well-lubricated billet is forced to pass through a die containing two equal cross section channels, being deformed by simple shear at the die channels intersection. The great advantage of the ECAP technique is related to the amount of plastic strain which can be continually imposed to the material after each pass through the die channels (Srinivasan, 2001).

The macroscopic understanding of the improvement in the mechanical properties of the materials deformed by ECAP requires the determination of the pressing force as well as the effective strains imposed after each pass. However, the works that present analytical solutions including the effects of work-hardening, die geometry and friction conditions in the pressing force and plastic strains calculations are limited to some specific process and material parameters. The first work was proposed by Segal (1995), in which an expression for the effective plastic strain, ε_{eq}, based upon the simple shear mechanism at the die channels intersection and the pressing pressure, *p*, can be obtained for a single ECAP pass as:

$$p=\sigma_y \varepsilon_{eq}=\frac{2\sigma_y}{\sqrt{3}}\cot(\Phi) \tag{1}$$

where σ_y and Φ are the billet uniaxial yield stress and the die channels intersection angle, respectively. Nonetheless, this expression neglects either the material work-hardening, since the material behaviour is assumed as rigid-plastic, or the friction effects at the die-billet interface.

Afterwards, Iwahashi *et al.* (1996) suggested an improvement to the effective plastic strain calculation which takes also into account the outer die curvature angle β:

$$\varepsilon_{eq}=\frac{1}{\sqrt{3}}\left\{\ 2\cot\left[\frac{\Phi+\beta}{2}\right]+\beta\ \operatorname{cosec}\left[\frac{\Phi+\beta}{2}\right]\ \right\} \tag{2}$$

The first analytical expression to the ECAP pressing force including the material work-hardening effect was proposed by Alkorta and Sevillano (2003) based upon the upper bound method together with a frictionless condition:

$$p=\frac{K}{(n+1)\sqrt{3}}\left\{2cot\left[\frac{\Phi+\beta}{2}\right]+\beta\right\}^{n+1} \tag{3}$$

where K and n are the Hollomon strength coefficient and the hardening exponent of the billet material, respectively. The friction effects on the ECAP pressure were first presented by Pérez (2004 a) by using the upper bound method, considering also the die geometric parameters, however, for a rigid-perfectly plastic material:

$$p=\frac{2\sigma_y}{\sqrt{3}}\left[mcot\left(\frac{\Phi}{2}\right)+\frac{m(l_E+l_S)}{d}+\frac{R\ m(\pi-\Phi)}{d}\right] \tag{4}$$

where m, d, R, l_E and l_S are the Tresca friction factor, the channels width, the outer die radius, the instantaneous billet length at the deformation surface entry and the billet length at the deformation surface exit, respectively.

Recently, Eivani and Karimi Taheri (2007) presented the first upper bound solution to the ECAP pressure in which the die geometric parameters, friction conditions and work-hardening behaviour were taking into account, defined by:

$$p=\frac{\sigma_y(1+m)}{\sqrt{3}}\left\{2cot\left[\frac{\Phi+\beta}{2}\right]+\beta\right\}+\frac{4m}{\sqrt{3}}\frac{(l_E+l_S)}{d} \tag{5}$$

Although the solution proposed by Eivani and Karimi Taheri (2007) considers the effects of the rheological and tribological parameters upon the ECAP pressure, this is restricted to a specific die geometry composed by only one fillet radius placed at the die bottom channels intersection. In view of the brief review presented here above, a more flexible solution is needed to obtain a complete analytical approximation for the pressure and or load during the ECAP method, as well as for the effective plastic strains after each pass of the billet through the die channels. In this context, the present work aims at providing a solution which takes also into account the effects of the different fillet radii, namely, the inner radius and the outer radius at the die channels intersection. The general solution based upon the upper bound method is firstly detailed wherein the equations for the force or pressure and effective plastic strains resulting from the ECAP deformation technique are presented. Then, the predictions determined with this general solution are compared to the analytical predictions and experimental results obtained by Eivani and Karimi Taheri (2007).

2. ANALYTICAL MODELING

The upper bound method (Kobayashi *et al.*, 1989) was adopted in the analytical modeling to obtain the expressions for the pressing force and the effective plastic strains, based on the die geometry schematically depicted in the Fig.1. This geometry, similar to the one proposed by Pérez (2004 b), considers different fillet radii at the die channels intersection. The outer fillet radius (R_{ext}) is placed in the bottom intersection while the inner (R_{int}) is located in the top region. In this figure, a square element (abcd) in the Region I of the billet moves as a rigid body with velocity V_0 towards the Region II which begins at the inlet surface (Γ_i) and ends at the outlet surface (Γ_o). This region corresponds to the deformation zone wherein severe plastic strains are imposed to the billet through a pure shear deformation mode. As the deformed element a'b'c'd' crosses Γ_o, it moves in the Region III similarly as in the Region I. Some important aspects inherent to the Fig.1 are the origin of the rectangular coordinate system taken in the point O with x and y axes positive values to the left and down, respectively. In this point also is placed the origin of the cylindrical coordinates system (r, θ, z). In the deformation zone it is assumed that the billet moves along circular paths with center at O. The β angle delimitates the Region II while δ is either the angle between Γ_i and the velocity vector V_0 or Γ_o and V_0 in the Region III. The symbol Φ represents the channels intersection angle, L is the width of the channels and γ is the amount of shear strain imposed to the billet at each pass through Region II.

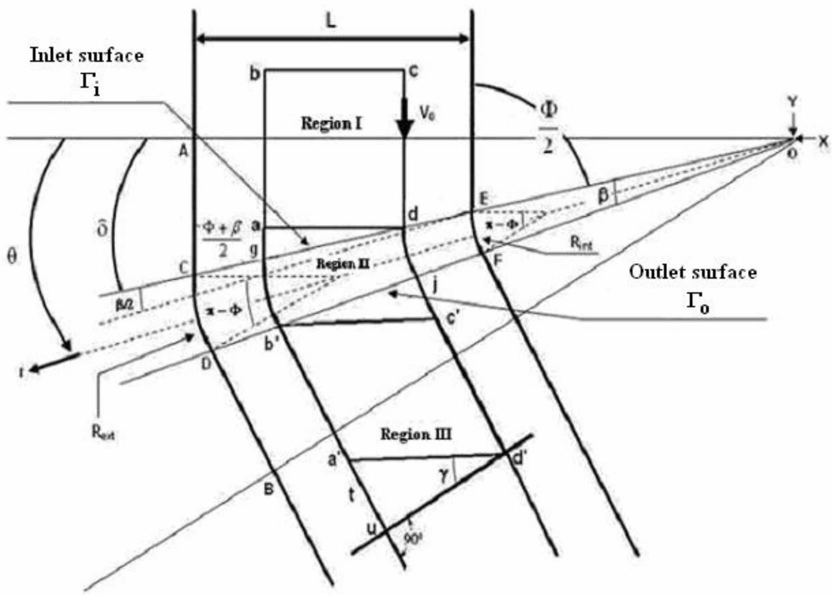

Figure 1. Deformation geometry of the ECAP process considered in the present work.

The upper bound method is based on the virtual works principle providing a maximum value to the work rate dissipated on a certain surface. In plasticity problems, for instance, in metal forming analysis, this upper limit is achieved by considering a kinematically admissible velocity field that satisfies both incompressibility and velocity boundary conditions. Thus, the energy portion dissipated by the external forces is equated to that resulting from the plastic deformation process. According to Kobayashi *et al.* (1989), the upper bound method can be defined as:

$$\int_V \sigma_{ij}^* \dot{\varepsilon}_{ij}^* dV + \int_{S_D} \kappa \left| \Delta v^* \right| dS - \int_{S_F} F_i v_i^* dS \geq \int_{S_u} F_i v_i dS \tag{6}$$

where,

v_i^* is a kinematically admissible velocity field;

$\dot{\varepsilon}_{ij}^*$ is a strain rate field derivable from v_i^*;

$\left| \Delta v_i^* \right|$ is the amount of velocity discontinuity along the surface S_D;

σ_{ij}^* is the Cauchy stress tensor associated to the strain-rate field $\dot{\varepsilon}_{ij}^*$;

κ is the pure shear yield stress;

F_i are the tensile stresses present in the tensile surface S_F and in the prescribed velocities surface S_u.

According to the upper bound method, the representation of the velocity hodographs is needed to obtain the solution for the kinematically admissible velocity field v_i*. The corresponding velocity hodographs at the ECAP die channel entry and exit surfaces are represented in Fig. 2. The velocity field can be defined in cylindrical coordinates (r, θ, z) from Fig. 2 by V_r,= 0, $V_\theta = V_0 \cos\delta$ and $V_z = 0$. From this velocity field, the only nonzero strain rate is due to the shear strain tensor component and can be determined by (Avitzur, 1968):

$$\dot{\varepsilon}_{r\theta} = \frac{1}{2}\left(\frac{1}{r}\frac{\partial V_r}{\partial \theta} + \frac{\partial V_\theta}{\partial r} - \frac{V_\theta}{r} \right) = -\frac{1}{2}\frac{V_0 cos\delta}{r} \tag{7}$$

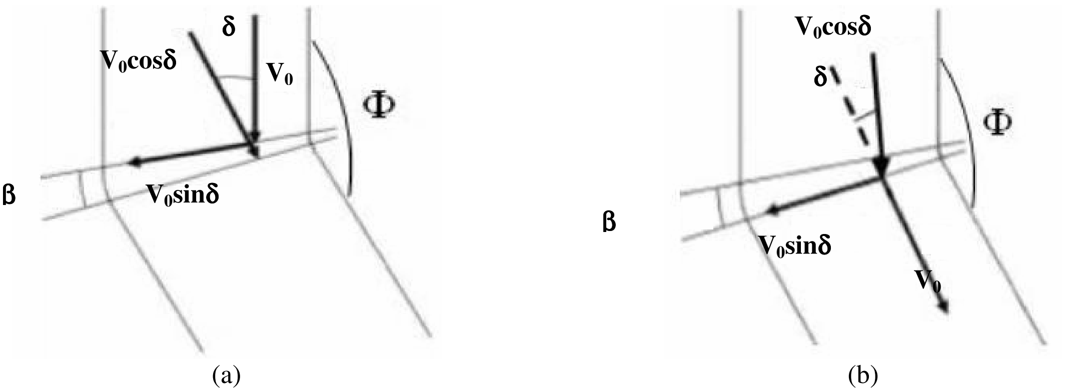

Figure 2. Velocity hodographs in the die deformation zone: (a) entry surface and (b) exit surface.

In order to establish the upper bound method, one needs to equate the external work rate to the internal work rate. Firstly, the external work rate is obtained by the action of the plunger on the billet, that is,

$$\dot{W}_{ext} = pL^2V_0 \tag{8}$$

where P and L are the ECAP pressure and the channels width respectively. On the other hand, the internal work is the sum of the contribution of the energy dissipated in the Regions I, II and III and at the billet-die contact surfaces, according to Fig.1, that is:

$$\dot{W}_{int} = \dot{W}_{DZ} + \dot{W}_{\Gamma_i} + \dot{W}_{\Gamma_o} + \dot{W}_{R_{ext}} + \dot{W}_{R_{int}} + \dot{W}_{AC} + \dot{W}_{DB} + \dot{W}_A + \dot{W}_B \tag{9}$$

where each term is defined as follows. First of all, the energy dissipated in the deformation zone (DZ) is given by:

$$\dot{W}_{DZ} = 2L\kappa \int_{\delta}^{\delta+[(\pi-\Phi)tan(\beta/2)cosec((\Phi+\beta)/2)]} \int_{R_{int}}^{R_{ext}} \dot{\varepsilon}\, rdrd\theta = L^2V_0\kappa\left[(\pi-\Phi)tan\left(\frac{\beta}{2}\right)cosec\left(\frac{\Phi+\beta}{2}\right)\right] \tag{10}$$

where the angle β is defined from Fig.1 by:

$$\beta = 2tan^{-1}\left\{\frac{(R_{ext}-R_{int})\,sin\Phi}{\left\{L^2+(R_{ext}-R_{int})^2\left[\cos^2(\Phi/2)-\sin^2\Phi\right]\right\}^{\frac{1}{2}}}\right\} \tag{11}$$

The energy dissipated at the inlet and outlet surfaces of the deformation zone are respectively approximated by:

$$\dot{W}_{\Gamma_i} = L\int_{R_{int}}^{R_{ext}} \kappa\left|\Delta v^*\right|dr = (R_{ext}-R_{int})L\kappa V_0 sin\delta = L^2\kappa V_0\, cot\left[\frac{\Phi+\beta}{2}\right] \tag{12}$$

$$\dot{W}_{\Gamma_o} = \dot{W}_{\Gamma_i} = L^2\kappa V_0\, cot\left[\frac{\Phi+\beta}{2}\right] \tag{13}$$

Conversely, the energy dissipated at the contact region between the billet and the outer fillet radius is equal to:

$$\dot{W}_{R_{ext}} = \int_{S_{ext}} Lm\kappa\left|v^*_{R_{ext}}\right|dS = Lm\kappa V_0 S_{R_{ext}} = L^2 m\kappa V_0\beta \tag{14}$$

where m is the friction factor, $|v^*_{Rext}|$ is the velocity discontinuity in the deformation zone and S_{Rext} is the outer arc length in the Region II defined as $S_{Rext}= (R_{ext} - R_{int})\ \beta$. In the same way, the energy dissipated at the contact region between the billet and the inner fillet radius is given by:

$$\dot{W}_{R_{int}} = \int_{S_{int}} Lm\,\kappa\left|v^*_{R_{int}}\right|dS = Lm\,\kappa\, S_{R_{int}}V_0 cos\,\delta = \frac{L^2 m\kappa\, V_0 R_{int}\,\beta}{(R_{ext}-R_{int})} \tag{15}$$

where S_{Rint} is the inner arc length in the Region II defined as $S_{Rint}= R_{int}\ \beta$.

The energies dissipated due to the contact between the billet and the die in the regions AC and DB are given by:

$$\dot{W}_{AC} = \dot{W}_{DB} = \int_{S_{AC}} m\kappa \left| v_{AC} \right| dS = m\kappa V_0\, S_{AC} = Lm\, \kappa V_0\, AC = L^2 m\kappa V_0\, tan\delta = L^2 m\kappa V_0 cot\left[\frac{\Phi+\beta}{2}\right] \tag{16}$$

As well, the energies due to the contact between the billet and the regions located before and after the points A and B respectively are given by:

$$\dot{W}_A = 4\int_{S_A} m\kappa \left| v_A \right| dS = 4m\kappa V_0 S_A = 4Lm\kappa V_0 h_A \tag{17}$$

$$\dot{W}_D = 4\int_{S_B} m\kappa \left| v_B \right| dS = 4m\kappa V_0 S_B = 4Lm\kappa V_0 h_B \tag{18}$$

where S_A and S_B are the contact area before and after the points A and B defined by product between the corresponding current lengths of the billet h_A and h_B and the die channel width L, respectively. Finally, the internal work rate after one single ECAP pass is obtained by the sum of Eq. (10) and Eqs. (12-18) as:

$$\dot{W}_{Int} = 2L^2 V_0 \kappa \left\{ (m+1) cot\left[\frac{\Phi+\beta}{2}\right] + \frac{m\beta}{2}\left[1+\frac{R_{int}}{(R_{ext}-R_{int})}\right] + 2m\kappa V_0 \left(\frac{(h_A+h_B)}{L}\right) + \frac{(\pi-\Phi)}{2} tan\left[\frac{\beta}{2}\right] cosec\left[\frac{\Phi+\beta}{2}\right] \right\} \tag{19}$$

Then, the ECAP pressure normalized by the uniaxial yield stress σ_y is obtained by comparing Eqs. (8) and (19):

$$\frac{p}{\sigma_y} = \frac{2}{\sqrt{3}} \left\{ (m+1) cot\left[\frac{\Phi+\beta}{2}\right] + \frac{m\beta}{2}\left[1+\frac{R_{int}}{(R_{ext}-R_{int})}\right] + 2m\frac{(h_A+h_B)}{L} + \frac{(\pi-\Phi)}{2} tan\left[\frac{\beta}{2}\right] cosec\left[\frac{\Phi+\beta}{2}\right] \right\} \tag{20}$$

where according to the von Mises yield criterion the pure shear yield stress $\kappa=\sigma_y/\sqrt{3}$. Or, in terms of ECAP load P:

$$P = \frac{2L^2\sigma_y}{\sqrt{3}} \left\{ (m+1) cot\left[\frac{\Phi+\beta}{2}\right] + \frac{m\beta}{2}\left[1+\frac{R_{int}}{(R_{ext}-R_{int})}\right] + 2m\frac{(h_A+h_B)}{L} + \frac{(\pi-\Phi)}{2} tan\left[\frac{\beta}{2}\right] cosec\left[\frac{\Phi+\beta}{2}\right] \right\} \tag{21}$$

Analyzing the Eqs. (20) and (21) it is worth to note an indetermination when $R_{ext} = R_{int}$. In the limit $(R_{ext} - R_{int}) \to 0$, the solutions to both ECAP normalized pressure (p) and load (P) are obtained by applying the L'Hôpital's theorem as:

$$\frac{p}{\sigma_y} = \frac{2}{\sqrt{3}} \left\{ (m+1) cot\left[\frac{\Phi+\beta}{2}\right] + \frac{mR_{ext}}{L}\sin\Phi + 2m\frac{(h_A+h_B)}{L} \right\} \tag{22}$$

$$P = \frac{2\sigma_y}{\sqrt{3}} \left\{ (m+1) cot\left[\frac{\Phi+\beta}{2}\right] + \frac{mR_{ext}}{L}\sin\Phi + 2m\frac{(h_A+h_B)}{L} \right\} \tag{23}$$

which can be reduced to the solution obtained by the ideal work method for the frictionless condition by setting $m = 0$, as shown by Pérez (2004 a).

The total effective plastic strain during the ECAP process is determined by the sum of effective plastic strains in the deformation zone and at the entry and exit surfaces. Therefore,

$$\varepsilon^p_{eq} = \frac{1}{\sqrt{3}}\gamma_{DZ} = \frac{1}{\sqrt{3}} \left\{ 2cot\left[\frac{\Phi+\beta}{2}\right] + (\pi-\Phi)\ tan\left(\frac{\beta}{2}\right) cossec \left[\frac{\Phi+\beta}{2}\right] \right\} \tag{24}$$

which is corrected by the von Mises yield criterion applied to the case of pure shear where γ_{DZ} represents the shear strain required to deform the square element abcd to a'b'c'd' (see Fig.1). On the other hand, the uniaxial yield stress σ_y is defined from as the mean flow stress σ_m adopting the Swift's work-hardening law:

$$\sigma_y = \sigma_m = \frac{1}{\varepsilon^p_{eq}} \int_0^{\varepsilon^p_{eq}} \left[K(\varepsilon_0 + \varepsilon^p)^n \right] d\varepsilon^p \tag{25}$$

where ε_0 is pre-strain term whereas ε^p stands for the plastic strain.

The analytical solutions proposed in the present work were implemented in Fortran90® language. The analytical studies were carried out at room temperature neglecting the heating due to the friction in the billet-die contact interface. Furthermore, the billet material behavior is considered as isotropic described by the von Mises plasticity yield criterion. Firstly, the results obtained with the present model were compared to the predictions determined from the upper bound solution proposed by Eivani and Karimi Taheri (2007) for $V_0 = 0.05$ mm/s, $R_{int} = 0$ mm and $R_{int} = 10$ mm. Two friction conditions were adopted by assuming m equals to 0 and 0.17. In addition, the R_{ext} was assumed to vary in the interval between 0 and10 mm together with a fixed intersection die channels angle Φ equals to 90°. In this study, the material adopted is an IF-steel which work-hardening behavior is described from the uniaxial tensile test by Eq. (25) with $\varepsilon_0 = 0.004852$, K= 544.958 MPa and n=0.235. Finally, the experimental ECAP load data determined by Eivani and Karimi Taheri (2007) for an Al-6070 with $\varepsilon_0 = 0$, K = 179.3 MPa and n = 0.26 is evaluated for $\beta = 0^0$ and 30^0 and m = 0.18.

3. RESULTS AND DISCUSSION

Figure 3 compares the normalized pressing pressures predicted by the present work and those from Eivani and Karimi Taheri (2007) for $\Phi = 90°$as a function of the outer angle β. The material considered is the IF-steel which mechanical properties are defined by Eq. (25). Firstly, it is possible to note that the normalized pressure increases with the friction factor m for either solutions. Secondly, when $\beta = 0$ rad, i.e., for $R_{ext} = R_{int}$ 0 mm, the predictions from the proposed solution are identical to the solution of Eivani and Karimi Taheri (2007). Nevertheless, as R_{ext} tends to the maximum value considered (10 mm), the normalized pressure determined by the present solution is higher than the prediction obtained with the model of Eivani and Karimi Taheri (2007), due to the positive influence of the second term of the shear strain calculation at the deformation zone, γ_{DZ}, see Eq. (24). Thus, the analytical model of Eivani and Karimi Taheri (2007) can be retrieved as a particular case of the solution proposed in the present work. Actually, an increase of the angle β or, equivalently, of the outer radius R_{ext}, leads to a decrease of the shearing in the deformation zone and, thus, of the normalized pressure. In relation to the friction effects on the normalized pressure, one should observe that for m = 0.17, the normalized pressure values are practically two times higher than to the frictionless condition, as shown in Fig. 3(b). Clearly, this is due to dependence upon the friction factor m in the Eqs (20) and (22). It is worth noting that the values obtained from the model proposed by Eivani and Karimi Taheri (2007) are almost insensitive to the outer radius R_{ext}. This result contradicts the expected trend where an increasing ECAP pressure might be obtained as the R_{ext} value tends to zero.

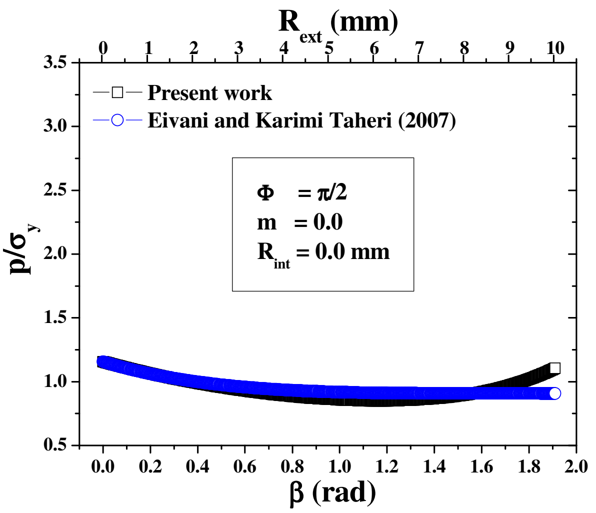

(a)

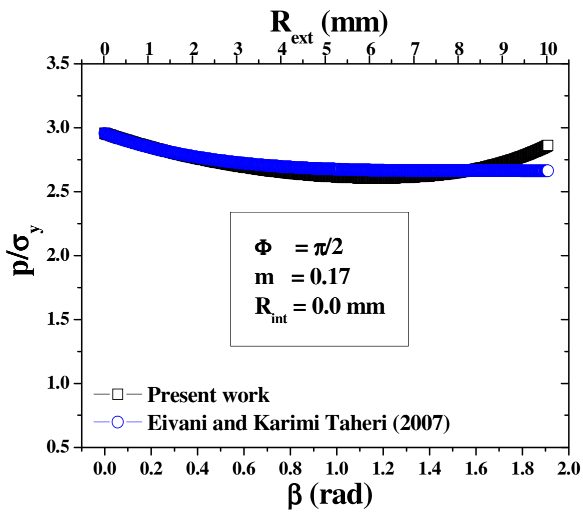

(b)

Figure 3. Normalized pressure determined for $\Phi = \pi/2$ as a function of the angle β: (a) m = 0 and (b) m = 0.17.

On the other hand, Figure 4 compares the effective plastic strain obtained as a function of the angle β for an intersection die channels angle $\Phi = 90$º. For the β–values between ~ 0.3 and $\pi/2$ rad, the present model predicts smaller effective plastic strains than the results calculated with the solution proposed by Eivani and Karimi Taheri (2007). In fact, the effective strain defined by Eq. (24) has two trigonometric terms which, in turn, closely depends upon the angle β as depicted in Fig. 4(b).

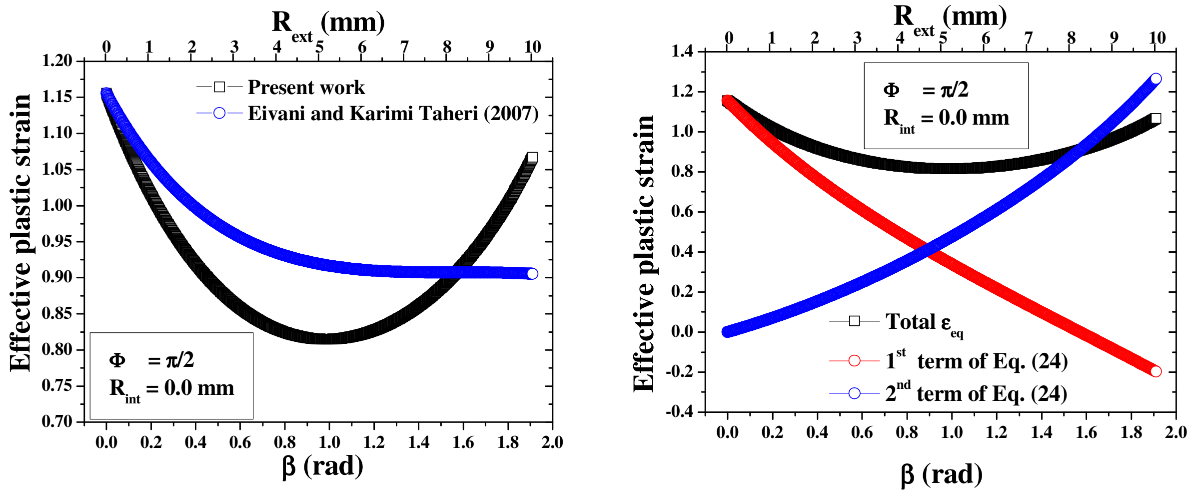

(a) (b)

Figure 4. Effective plastic strain as a function of the outer die curvature angle β or the outer fillet radius R_{ext}: (a) comparison with the prediction determined with the model proposed by Eivani and Karimi Taheri (2007) and (b) terms of the present solution given by Eq. (24).

Figure 5 presents the behavior of the normalized pressing pressure when the inner die fillet radius R_{int} is varied over a range of 0 to R_{ext} = 10 mm together with different values of the intersection die angle Φ. The friction effects are also considered by adopting m equals to 0 and 0.17, Figures 5 (a) and (b) respectively. For all Φ–values, the normalized pressing pressure increases with the friction factor m. Moreover, it is possible to observe two fundamental aspects. Firstly, the highest normalized pressure values are achieved for $\Phi = 90^0$ independently of the adopted friction factor m. Actually, for fixed and different values of the inner and outer die fillet radii ($R_{int} \neq R_{ext}$) the β angle has a maximum value for $\Phi = 90^0$, see Eq. (11). Otherwise, a maximum of the shear strain in the deformation zone γ_{DZ} and, therefore, of the effective strains, as shown in Fig. (6). Secondly, all the normalized pressing pressure curves decrease with an increase of the inner die fillet radius, R_{int}, or equivalently with a decrease in the difference between the die fillet radii, namely, in the ($R_{ext} - R_{int}$) value in Eq. (11). From this theoretical analysis, larger effective strains per ECAP pass, imposed to the billet by means of a deformation mode close to pure shear, ε^p_{eq} about to 1.15 in Fig. (6) for $\Phi = 90^0$, can be achieved when β is zero, that is, $R_{int} = R_{ext}$.

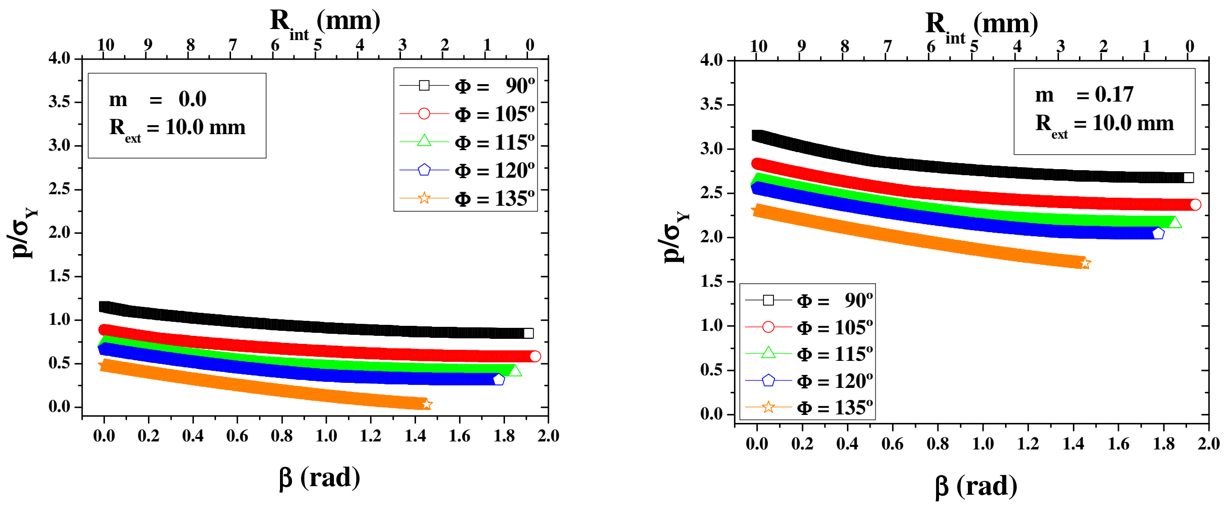

(a) (b)

Figure 5. Normalized ECAP pressure as a function of geometrical parameters: (a) m = 0 and (b) m = 0.17.

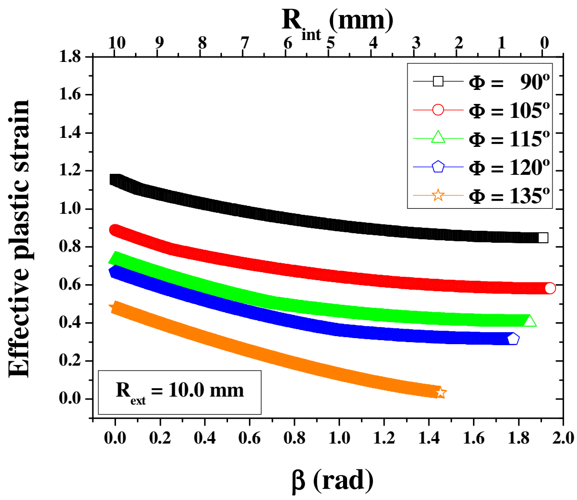

Figure 6. Effective plastic strains as a function of the Φ, R_{int} and β.

Figure 7 compares the ECAP load predicted by Eqs. (21) and (23) with the experimental values measured for an Al-6090 alloy by Eivani and Karimi Taheri (2007) for different values of Ψ (or equivalently β) and for a constant friction condition. In the first case, where $\Psi = \beta = 0°$, the theoretical predictions are identical and higher than the experimental value. Conversely, when the outer angle Ψ (or β) is near to 30°, the ECAP load predicted by the present solution is closer to the experimental load than the corresponding prediction obtained with the model proposed by Eivani and Karimi Taheri (2007). This difference is due to the fact that the angle β is calculated as a function of the die geometry which includes the effects of different fillet radii, see Eq. (11). In the model developed by Eivani and Karimi Taheri (2007) the angle Ψ is a known constant parameter neglecting the dependence upon the die geometry. Besides, it should be noted that there is a coupling between the rheological material parameters, described here by an exponential law from the uniaxial tensile behaviour, and the tribological effects at the billet-die interfaces which are accounted for by means of a single parameter, namely, the friction factor m. The m-value has been taken equal to 0.18 and corresponds to Coulomb friction μ of about 0.10. In the ECAP process, the stress range of interest varies nearly between the plane-strain compression and pure shear. Hence, the choice of the effective stress-strain measures based upon the von Mises isotropic yield criterion should correctly describe the work-hardening behavior of the billet. For F.C.C. metals such as the Al-6070 alloy evaluated in the work conducted by Eivani and Karimi Taheri (2007), it is well known that the corresponding yield surfaces either determined experimentally or by means of polycrystalline plasticity models lies between the Tresca and the von Mises (Barlat, 1987). Lastly, an improved solution could be achieved by considering a more refined distribution of the velocity hodographs within the die deformation zone, see Fig. (2).

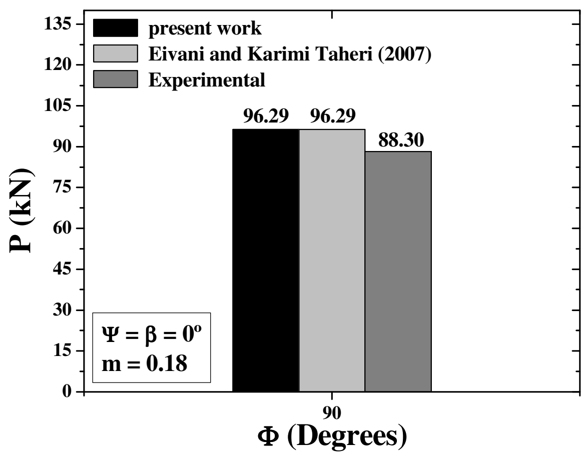

(a)

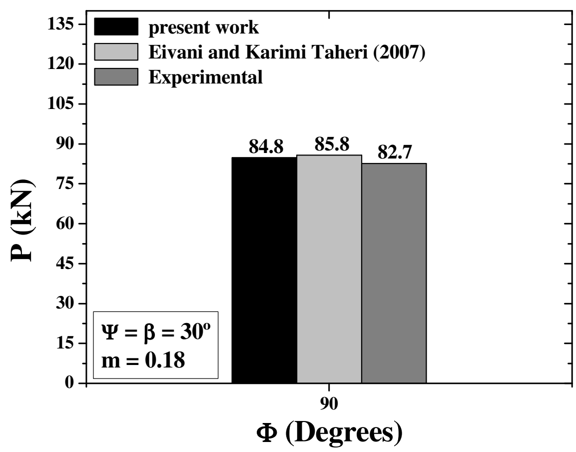

(b)

Figure 6. Predicted and measured ECAP loads obtained for an Al-6090: (a) $\Psi = 0°$ and (b) $\Psi = 30°$.

4. CONCLUSIONS

From the analytical solution based upon the upper bound method proposed in this work for the ECAP process and the corresponding theoretical analyses, some concluding remarks can be outlined:

1) The upper bound model proposed to approximate the ECAP pressing pressure and the resulting effective plastic strain may be considered as a more rigorous solution since all the contributions describing the work-rates dissipated along the ECAP process have been fulfilled. Also, this solution is more pertinent vis-à-vis the geometrical parameters of the ECAP die, namely, the consideration of either the inner and or the outer die fillet radii together with the friction and the work-hardening of the billet.

2) Concerning the effects of the die fillet radii, the proposed model predicts more consistent trends for the normalized pressing pressure in the cases where either the outer die fillet radius R_{ext} tends to zero or when its difference with respect to the inner die fillet radius, $(R_{ext} - R_{int})$, becomes very small.

3) The conducted theoretical analysis shows that larger effective strains per ECAP pass, ε^{p}_{eq}, about to 1.10 for $\Phi = 90^0$, could still be achieved with larger β angles along with a significant reduction in the normalized pressing pressure in comparison to sharper inner die fillet radii values. This result is very interesting since the disadvantages related to the increasing loads needed for the multi-pass ECAP process could be minimized by using different die geometries.

4) The proposed model predicts more realistic ECAP loads for an Al-6070 alloy in comparison to the analytical solution of Eivani and Karimi Taheri (2007). This is directly associated to the rigorous upper bound solution adopted which considers the effects of the die geometrical parameters in the calculation of the effective plastic strain during the ECAP process.

5. ACKNOWLEDGEMENTS

Neil de Medeiros thanks to CAPES for the PhD. research scholarship. Luciano P. Moreira is grateful to the research grant from the CNPq (Project No. 400609/2004-5 “Novas ligas estruturais para a indústria automobilística”).

6. REFERENCES

Alkorta, J. and Sevillano, J.G., 2003,“A comparison of FEM and upper-bound type analysis of equal-channel angular pressing (ECAP)”, Journal of Materials Processing Technology, Vol.141, pp.313-318.

Ansys User’s Manual for Revision 5.0, 1994, Swanson Analysis Systems Inc.

Avitzur, B., 1968, “Metal Forming: Processes and Analysis”. Mc Graw-Hill Publishing Company Ltd., New Delhi.

Barlat F., 1987, “Crystallographic texture, anisotropic yield surface and forming limits of sheet metals”, Materials Science and Engineering, Vol. 9, pp.55-72.

Eivani, A.R. and Karimi Taheri, A., 2007, “An upper bound solution of ECAE process with outer curved corner”, Journal of Materials Processing Technology, Vol.182, pp. 555–563.

Iwahashi, Y., Wang,W., Nemoto, M. and Langdon, T.G., 1996, “Principle of equal-channel angular pressing for the processing of ultra-fine grained materials”, Scripta Materialia, Vol.35, pp. 143-46.

Kobayashi, S., Oh, S.I. and Altan, T., 1989, “Metal Forming and the Finite-Element Method”, Oxford University Press, New York.

Pérez, C.J.L., 2004 a, “Upper bound analysis and FEM simulation of equal fillet radii angular pressing”, Modelling and Simulation in Materials Science and Engineering, Vol.12, pp.205-214.

Pérez, C.J.L., 2004 b, “On the correct selection of the channel die in ECAP processes”, Scripta Materialia, Vol.50, pp.387-393.

Segal, V.M, 1995, “Materials processing by simple shear”, Materials Science and Engineering A, Vol. 197, pp. 157-64.

Srinivasan, R., 2001, “Computer simulation of the equichannel angular extrusion (ECAE) process”, Scripta Materialia, Vol.44, pp. 91-96.

Valiev, R.Z., Islamgaliev, R.K. and Alexandrov, I.V., 2000, “Bulk nanostructured materials from severe plastic deformation”, Progress in Materials Science, Vol.45, pp. 103-89.

Valiev, R.Z. and Langdon, T.G., 2006, “Principles of equal-channel angular pressing as a processing tool for grain refinement”, Progress in Materials Science, Vol.51, pp. 881-981.

Zhao, G., Xu, S., Luan, Y., Guan, Lun, N. and Ren, X., 2006, “ Grain refinement mechanism analysis and experimental investigation of equal channel angular pressing for producing pure aluminum ultra-fine grained materials”, Materials Science and Engineering A, Vol.437, pp. 281-292.

Zhang, Z.J., Son, I.H., Im, Y.T., Park, J.K., 2007, “Finite element analysis of plastic deformation of CP-Ti by multi-passs equal channel angular extrusion at medium hot-working temperature”, Materials Science and Engineering A, Vol.447, pp. 134-141.

7. RESPONSIBILITY NOTICE